Results in Engineering 24 (2024) 102816

Contents lists available at ScienceDirect

Results in Engineering

journal homepage: www.sciencedirect.com/journal/results-in-engineering

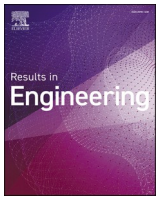

Fuzzy logic-based particle swarm optimization for integrated energy management system considering battery storage degradation

Oladimeji Ibrahim [a,b], Mohd Junaidi Abdul Aziz [a,*], Razman Ayop [a], Ahmed Tijjani Dahiru [a,c], Wen Yao Low [a], Mohd Herwan Sulaiman [d], Temitope Ibrahim Amosa [e]

[a] Power Electronics and Drive Research Group (PEDG), Faculty of Electrical Engineering, Universiti Teknologi Malaysia, Johor Bahru, 81310, Johor, Malaysia
[b] Department of Electrical and Electronics Engineering, University of Ilorin, Ilorin, 240003, Nigeria
[c] Department of Electrical/Electronics Technology, Federal College of Education (Technical) Bichi, PMB 3473, Kano, Nigeria
[d] Faculty of Electrical & Electronics Engineering Technology, Universiti Malaysia Pahang Al-Sultan Abdullah (UMPSA), Pekan Pahang, Malaysia
[e] Department of Electrical and Electronics Engineering, Universiti Teknologi PETRONAS, 32610, Seri Iskandar, Perak, Malaysia

ARTICLE INFO

Keywords:
Fuzzy logic
Particle swarm optimization
Energy management system
Battery degradation
Solar PV system

ABSTRACT

Considering the rapidly evolving microgrid technology and the increasing complexity associated with integrating renewable energy sources, innovative approaches to energy management are crucial for ensuring sustainability and efficiency. This paper presents a novel Fuzzy Logic-Based Particle Swarm Optimization (FLB-PSO) technique to enhance the performance of hybrid energy management systems. The proposed FLB-PSO algorithm effectively addresses the challenge of balancing exploration and exploitation in optimization problems, thereby enhancing convergence speed and solution accuracy with robustness across diverse and complex scenarios. By leveraging the adaptability of fuzzy logic to adjust PSO parameters dynamically, the method optimizes the allocation and utilization of diverse energy resources within a grid-connected microgrid. Under fixed grid tariffs, the investigation demonstrates that FLB-PSO achieves grid power purchase and battery degradation costs of $1935.07 and $49.93, respectively, compared to $2159.67 and $61.43 for the traditional PSO. This results in an optimal cost of $1985.00 for FLB-PSO, leading to a cost saving of $236.09 compared to the $2221.10 of PSO. Furthermore, under dynamic grid tariffs, FLB-PSO incurs grid power purchase and battery degradation costs of $2359.20 and $64.66, respectively, in contrast to $2606.47 and $54.61 for PSO. The optimal cost for FLB-PSO is $2423.86, representing a cost reduction of $237.23 compared to the $2661.08 of PSO. The FLB-PSO algorithm proficiently manages energy sources while addressing complexities associated with battery storage degradation. Overall, the FLB-PSO algorithm outperforms traditional PSO in terms of robustness to system dynamics, convergence rate, operational cost reduction, and improved energy efficiency.

1. Introduction

1.1. Study background

There is global consensus on increasing the proportion of renewable energy-based power generation in the overall energy mix, shifting to a more environmentally friendly power generation [1]. Over the past three decades, there has been substantial growth in deploying renewable energy sources like solar photovoltaic, wind, hydroelectricity, and biomass. Governments and organizations are offering incentives to promote the adoption of renewable energy technologies to combat global climate change, decrease greenhouse gas emissions, and improve energy security [2,3]. The initiatives have resulted in significant advancements in incorporating renewable energy sources into the existing power grids. This increasing integration of renewable energies reduces reliance on fossil fuels, addresses air pollution concerns, and promotes sustainable energy supply to meet continuous demand growth. Expansion of renewable energy has significantly contributed to diversifying energy sources, improving resilience, and creating economic opportunities for stakeholders [4].

However, the increasing incorporation of renewable energy sources (RES) such as solar PV and wind power into the existing grid network presents challenges due to their irregular nature and wide distribution. Nonetheless, progress in energy storage technologies, power interface advancement, smart grid infrastructure, and advanced energy control

* Corresponding author.
E-mail address: junaidi@utm.my (M.J. Abdul Aziz).

https://doi.org/10.1016/j.rineng.2024.102816
Received 4 July 2024; Received in revised form 14 August 2024; Accepted 29 August 2024
Available online 30 August 2024

List of acronyms

GW	Gigawatts
kWh	kilowatt-hours
IEA	International Energy Agency
PV	Solar photovoltaic
RES	Renewable energy sources
EMS	Energy management systems
AI	Artificial intelligence
BESS	Battery energy storage system
FLC	Fuzzy logic controller
FLB-PSO	fuzzy logic-based particle swarm optimization
MPC	Model predictive control
PSO	Particle swarm optimization
GA	Genetic algorithms
SA	Simulated annealing
TS	Tabu search
FPA	Flower pollination algorithm
TOU	Time-of-use
SoC	State of charge
AC	Alternating current
ANN	Artificial neural networks
RL	Reinforcement learning
DR	Demand response
DE	Differential evolution
PVGIS	Photovoltaic geographical information system
COG	Center of gravity or area
MF	Membership function
RE	Relative error
AD	Average distance
MOM	Mean of maximum
FOM	First of maximum
MeOM	Mean of maxima (MeOM)
P & O	Perturb and observe
MPPT	Maximum power point tracker

strategies offer prospects for tackling these problems [3,5]. Adaptable grid management approaches are crucial for ensuring the dependable and effective integration of fluctuating renewable energy resources. The emergence of different energy management systems (EMS), including demand response, demand-side management, and utility-side energy regulation, have been playing significant roles in facilitating the seamless accommodation of renewables with minimal impact on grid stability. These advanced strategies are fundamental for maximizing the advantages of hybrid renewable energy, decreasing greenhouse gas emissions, and enhancing energy security. Developing flexible energy management strategies is essential as renewable RES becomes more widespread in the power system. These strategies must ensure a reliable energy supply while maintaining efficient demand management and optimizing the economic utilization of both renewable generation systems and grid power [6].

Recent developments in EMS technology aimed at maximizing the economic advantages of RES now employ advanced, sophisticated optimization techniques. The popular methods cover the linear and nonlinear programming methods, metaheuristic optimization algorithms, machine learning, and other artificial intelligence (AI) techniques for driving progress and innovations in EMS [7,8]. These methods have been adept at enhancing the efficiency and effectiveness of energy management strategies through real-time monitoring, predictive analytics, and adaptive control measures. Utilizing these innovative EMS tools in standalone and grid-connected hybrid energy systems has contributed significantly to improved grid flexibility, responsiveness, and system performance enhancement, as well as optimizing multiple energy systems regardless of their inherent stochastic nature. Deployment of efficient EMS has also contributed to grid stability and energy cost reduction, promoting hybrid energy deployment for peak load management while addressing battery energy storage system (BESS) degradation issues. Additionally, adopting EMS solutions has facilitated a shift towards a more sustainable and robust energy sector. These solutions provide a dynamic platform that aligns demand with supply, maximizes renewable energy utilization, and mitigates excessive generation.

To effectively fulfill energy management requirements in hybrid energy systems, EMS optimization methods must be capable of meeting the technical and operational challenges associated with the inherent features of diverse energy resources and deployment environments. Operationally, EMS deployment faces hurdles concerning regulatory compliance, cybersecurity, and stakeholder acceptance [9]. On the technicality, hybrid energy systems possess inherent complexity involving various dynamic and stochastic processes, hindering the development of accurate and reliable EMS models. Hybrid energy systems often incorporate a diverse mix of renewable and non-renewable energy sources, grid systems, storage solutions, and irregular consumption patterns [10,11]. Therefore, designing EMS algorithms to effectively manage these variabilities requires substantial optimization capability, scalability, adaptability, robustness, and computational efficiency. Advanced EMS optimization algorithms aid the seamless integration of various energy sources, such as solar PV, wind, batteries, and the grid, while managing dynamic grid tariffs and demand response programs for cost-effective energy management and stability. EMS algorithms manage renewable generation variability and grid usage, optimize battery management, and enhance overall energy efficiency to maximize economic benefits. More importantly, they play a significant role in real-time decision-making, system scalability, flexibility, and accommodating any possible system expansions.

An EMS algorithm is designed to fulfill multiple tasks and objectives, often involving conflicting goals and unique operational constraints, making it challenging to develop a generally accurate and comprehensive model. To address these complexities, continuous research on advanced optimization algorithms becomes essential. In recent times, the most researched EMS algorithms include but are not limited to Particle Swarm Optimization (PSO), Genetic Algorithms (GA), Fuzzy Logic Control (FLC), Tabu Search (TA), and harmony search algorithm [10–13]. These algorithms are known for handling various levels of hybrid energy systems' linear, nonlinear, and dynamic nature. Nevertheless, they often face challenges such as convergence issues, computational complexity, and the need for careful parameter tuning. They must be carefully designed to handle uncertainties and highly stochastic environments effectively while ensuring scalability and robustness across various conditions. Additionally, integrating these algorithms with existing systems and balancing multi-objective optimization problems can be complex and time-consuming [9–11]. These challenges called for advanced computationally efficient EMS algorithms to meet the essential demands in hybrid energy systems with their inherent dynamic features.

In the past two decades, hybridization approaches that combine different algorithms have shown significant promise in enhancing the performance of EMS algorithms. These hybrid techniques leverage the strengths of various optimization methods to address the limitations innate in individual algorithms. For instance, combining PSO with ANN can improve convergence speed and solution accuracy by dynamically adjusting PSO parameters ANN [14]. Similarly, integrating GA with PSO can enhance exploration and exploitation capabilities, leading to more robust and efficient solutions [15]. Hybrid methods have effectively

managed the complexities of real-time decision-making, scalability, and adaptability in diverse and dynamic hybrid energy management systems. Combining multiple objectives, such as cost reduction, energy efficiency, and system reliability, hybrid algorithms offer more comprehensive and effective solutions for modern energy management challenges.

The PSO is considered one of the most extensively investigated optimization algorithms across diverse applications in recent years [10]. The traditional PSO often faces fundamental challenges that impact its performance in complex optimization problems, notably premature convergence, where the swarm rapidly converges around a local optimum, potentially missing the global one. More importantly, selecting appropriate values for PSO parameters, such as inertia weight and cognitive and social coefficients, is critical for the algorithm's efficient performance and, therefore, requires careful tuning to balance exploration and exploitation effectively [11,16]. Hybridizing PSO with other optimization methods, such as metaheuristics and machine learning techniques, can achieve effective parameters tunning to enhance its exploration and exploitation capabilities for better solution quality and robust optimal performance. These gaps in the literature underscore the necessity to advance further PSO variant methods that can effectively adapt the optimization process parameters in highly dynamic hybrid energy systems environment.

This study proposes an hybrid fuzzy logic-based PSO (FLB-PSO) energy management system algorithm for optimizing hybrid solar PV generation, storage battery, and the grid system while meeting the load demand with minimum operational cost. By hybridizing PSO and fuzzy logic inference, the EMS aims to minimize energy costs and maximize operational efficiency through optimal battery charging/discharging scheduling. The EMS operation effectively limits grid power purchases for optimal cost and enhanced battery management procedures, improving performance and extending the battery's lifespan for economic benefits. The Fuzzy logic controller (FLC) is employed to adjust the PSO cognitive and social acceleration coefficient parameters dynamically, balancing the algorithm's exploration and exploitation to provide a more reliable, accurate, and robust solution. The FLC adaptation is based on formulated fuzzy rules between the PSO process relative error and particle diversity as inputs, with the cognitive and social coefficients as outputs, resulting in adaptive PSO parameters suitable for an improved solution quality in a dynamic hybrid energy system environment. The proposed approach ensures the algorithm's rapid convergence by effectively varying the PSO acceleration factors according to the optimization progress. Additionally, the ability of the algorithm to adapt to changes within the optimization landscape enhances the algorithm's robustness across complex problem cases.

The key contributions of this study are as follows.

- Hybridizing fuzzy logic with the PSO algorithm to dynamically adapt PSO parameters during optimization to improve solution quality.
- Leveraging multiple PSO parameters as feedback to enhance the algorithm's exploration and exploitation capabilities, effectively addressing the challenges of excessive exploration and premature convergence.
- Developing the FLB-PSO EMS algorithm that adjusts its behaviour based on problem characteristics, ensuring effective solution quality across diverse and complex applications and changing system dynamics.
- Developing an EMS algorithm that exhibits greater stability and robustness in exploring larger search spaces and refining solutions.

The remaining part of the paper is structured as follows: Subsection 1.2 provides background information and a review of some popular optimization algorithms focusing on metaheuristics and hybrid optimization techniques. Section 2 explains the proposed hybrid FLB-PSO algorithm, covering the system modelling and implementation. Section 3 presents the performance evaluation results of the proposed algorithm and the discussion. Finally, Section 4 presents the conclusions and recommendations for future research work.

1.2. Literature review

Energy management optimization techniques are crucial in improving energy systems' efficiency, reliability, and sustainability across various domains, including power generation, distribution, and consumption. These techniques encompass diverse methods and algorithms to optimize the allocation, utilization, and control of energy resources to meet operational objectives while minimizing costs and environmental impacts. From conventional optimization algorithms to advanced metaheuristics and machine learning-based approaches, energy management optimization techniques offer versatile solutions in addressing hybrid energy systems' complex and dynamic nature [17]. This subsection discussed standard optimization techniques' fundamental concepts, challenges, and applications.

The energy optimization process involves systematically analyzing, modelling, and deploying energy optimization methods to enhance energy resources' operational efficiency and performance. Popular energy optimization techniques leverage classical mathematical algorithms, statistical methods, and advanced computational tools to address various aspects of energy system management, comprising but not limited to generation scheduling, demand-side management, grid management, renewable integration, and resource allocation [11] Considering component factors such as energy demand, energy supply, costs, energy constraints, and environmental conditions, energy management optimization techniques enable informed decisions that optimize the utilization of energy resources to achieve desired objectives.

In recent times, classical optimization algorithms such as the gradient descent approach, Newton's method, simplex method, gradient-based nonlinear programming, and mixed-integer linear programming methods have been extensively investigated in solving optimization problems [8]. However, while useful in many cases, these conventional methods have intrinsic restrictions that limit their applicability and performance in handling complex optimization problems. For example, gradient descent, a popular first-order optimization technique, may struggle with non-convex and multimodal objective functions, frequently converge to local optima, and has a slow convergence rate [18,19]. Similarly, Newton's method, a second-order optimization procedure, requires a differentiable objective function and may experience convergence or numerical instability in high-dimensional or ill-conditioned optimization situations. These restrictions limit the effectiveness of gradient-based approaches in dealing with non-smooth or discontinuous objective functions, rendering them unsuitable for complex optimization problems [8,20].

There is continuously growing complexity in energy management problems necessitating the development of advanced control strategies, such as incorporating advanced computational intelligence and metaheuristic optimization algorithms. Also, hybrid approaches are increasingly being explored to achieve satisfactory solutions proficiently. Among the popular intelligent methods applicable in EMS are rule-based approaches such as fuzzy logic, expert systems, and decision trees [21–23]. these EMS methods employ predefined rules to regulate energy distribution within the hybrid energy systems. Such rules prioritize specific energy sources at certain times, for instance, the use of more solar PV energy during daylight hours and switch to wind energy at nighttime or grid electricity during low renewable generation [24]. Rule-based EMS provides simplicity, cost-efficiency, and customization options that facilitate easier implementation and comprehension than some of the advanced methods [25]Nevertheless, such strategies alone are incapacitated to dynamically adjust to the various factors affecting the hybrid energy system's components and operation. They frequently struggle to adapt to changing conditions, learn adequately, and improve without manual intervention.

To address some of the limitations of rule-based, heuristic

optimization techniques are progressively explored in energy management optimization, offering effective solutions to the inherent complexities and uncertainties. Techniques such as GA, SA, TS, and PSO have demonstrated the capability to tackle the dynamics of hybrid energy systems by efficiently exploring solution spaces [10,11]. Their dynamic operation enables adaptability in EMS, allowing them to respond promptly to fluctuations in energy demand, supply, and market conditions. At the same time, their scalability facilitates the management of small to medium-scale systems. By balancing exploring new solutions with exploiting known ones, heuristic algorithms are crucial in optimizing resource utilization and adhering to operational constraints. Incorporating probabilistic approaches and robust optimization strategies, these techniques have provided reliable EMS solutions under mild uncertain conditions [17].

However, applying heuristic methods in hybrid energy management optimization faces several challenges. Their performance is often highly dependent on parameter choices and initial conditions, which can lead to suboptimal solutions if not carefully tuned [8,10]. These methods often struggle with scalability, especially in complex systems with numerous variables and constraints, resulting in increased computational demands and longer processing times [10]. Heuristic approaches typically offer good solutions but are not guaranteed optimal, as they do not always exhaustively search the solution space. This limitation can lead to potential inefficiencies or missed opportunities for better optimal or quality solutions. Furthermore, balancing exploration and exploitation remains a significant challenge; excessive exploration can lead to longer convergence times, while excessive exploitation can cause premature convergence to suboptimal solutions. Moreover, heuristic methods often lack robustness and perform inconsistently under varying conditions, necessitating frequent adjustments or updates to maintain effectiveness.

Hybrid methods have emerged as a promising approach to overcoming prevailing challenges with independent heuristic methods and enhancing the accuracy of optimization solutions in energy management systems. Integrating multiple optimization techniques combines the strengths of different algorithms to address individual limitations and achieve a more robust and efficient solution. This synergetic approach leverages different heuristic techniques' exploratory and exploitation power alongside advanced methods, creating a more adaptable and comprehensive optimization framework. The hybridization approach has enhanced performance through dynamic parameter tuning, sequential hybridization, parallel hybridization, adaptability, and learning to handle uncertainties better and improve adaptability while addressing multiple objectives simultaneously [8,10,26]. Additionally, these methods often utilize multi-scale search strategies and adaptive mechanisms to refine the search process in response to real-time feedback, allowing for more accurate and robust solutions. This synergetic approach helps overcome individual algorithms' limitations, leading to more efficient and effective optimization in complex and dynamic environments.

Advanced hybrid optimization algorithms cut across strategies automated parameter tuning, online adaptive parameter tuning, and problem-specific adaptation for effective optimization in complex problems. Automated parameter tuning employs techniques such as combined metaheuristic algorithms, rule-based methods, and machine learning to dynamically adjust parameters, enhancing the adaptability and effectiveness of optimization processes [15,16,27]. Studies in this domain have demonstrated that such methods improve convergence and solution quality in energy management systems. These tailored methods manage nonlinearities and fluctuations in renewable energy sources, contributing to improved energy management efficiency and cost reduction, thus advancing the capabilities of hybrid optimization techniques in modern EMS. Largely, hybrid optimization approaches have shown great promise in addressing the complex stochastic nature of energy sources found in renewables, handling multi-objective optimization problems for optimal Pareto solutions, and advancing toward more intelligent and resilient energy management practices. Therefore, research on parameter tuning within hybrid energy system optimization is essential for developing robust, efficient, and adaptable EMS algorithms that meet the technical and operational challenges of diverse energy resources and deployment environments.

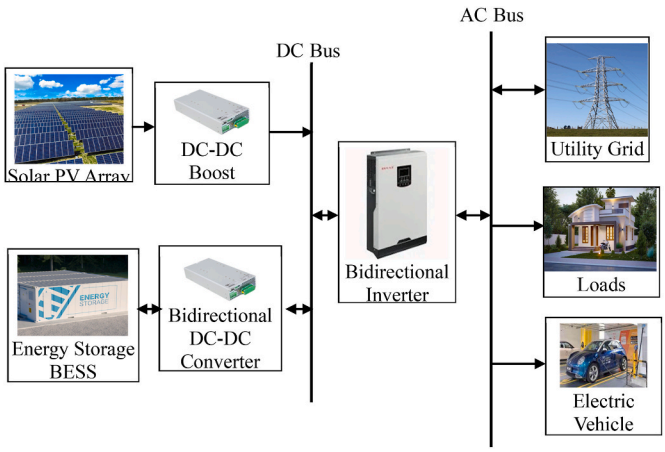

Fig. 1. Microgrid architecture.

2. Methodology

This study's proposed FLB-PSO EMS algorithm aims to manage an AC microgrid system comprising the conventional grid, which provides reliable power, and the solar PV source that supplies much of the daytime energy needs. The EMS is a vital component of the hybrid energy system that optimally manages the power generation sources, storage units, and electricity distribution to various loads, considering fixed and dynamic time-of-use (TOU) grid tariffs.

(a) System Configuration

As depicted in Fig. 1, the proposed microgrid system configuration incorporates multiple energy sources, power interfaces, and loads. The BESS balances the demand-supply dynamics, stores excess renewable energy generation, and reduces operational costs during peak hours. The solar PV and BESS units are connected to a DC bus, which is then connected to an AC bus via appropriate power electronic converters, as illustrated in Fig. 1. The AC distribution bus voltage is designed for an 11 kV, 50 Hz system.

(b) Load and Weather Profile

The study area is residential in Ilorin town, Kwara State, Nigeria, with coordinates 8.5373° N, 4.5444°. The location presently gets its total supply from the conventional grid. Considering the abundance of solar irradiance providing 5.5 kWh/m^2 energy in a day [28], incorporating solar PV systems to reduce energy costs becomes a viable option. The location, with around 750 housing units, primarily houses consumers with diverse energy demands and facilities, including cooling, heating, home appliances, lighting, and electronic equipment. To acquire the daily load profile, the daily consumption pattern over a month was recorded for three types of housing units, namely: 3-bedroom, 2-bedroom bungalow flats, and 4-bedroom duplex flats. The electrical load data was collected using a standard Fluke 434-II Power Quality and Energy Analyzer with hourly resolution. The collected energy data were averaged to obtain daily hourly demand, which was, in turn, scaled up for the total 750 housing units in the community, as shown in Fig. 2. The daily average minimum load demand was 458 kWh, and the peak energy demand stood at 957 kWh.

The location daily solar irradiance and ambient temperature data for

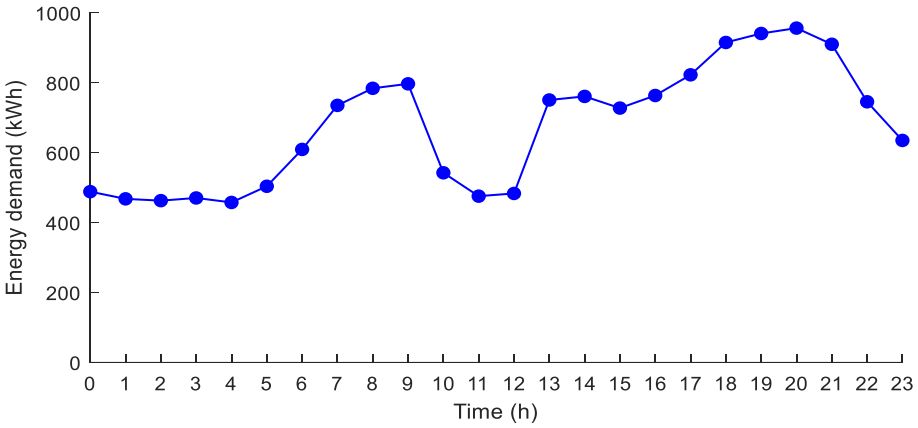

Fig. 2. Typical average daily load profile.

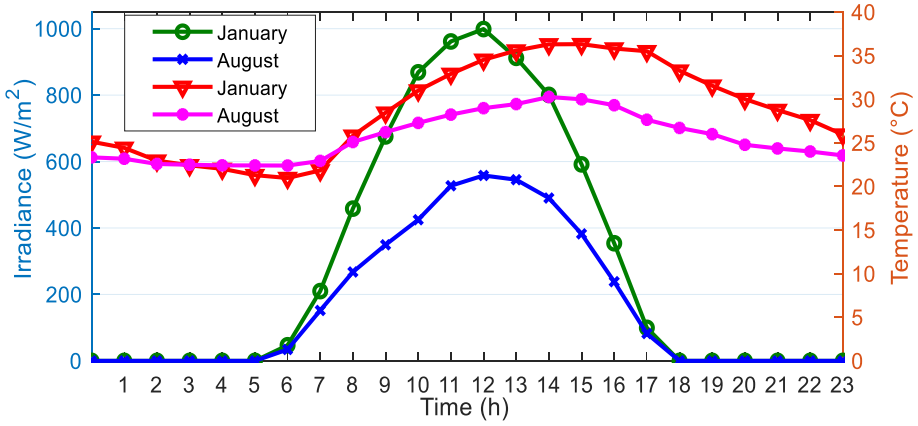

Fig. 3. Monthly daily average solar irradiance (W/m^2) and temperature (degree °C).

some months of the year were obtained from the Photovoltaic Geographical Information System (PVGIS) hosted by the European Commission [29]. Based on satellite data and reanalysis, the average solar irradiance data comprised average values for every hour from 2001 to 2024. Fig. 3 shows the months with the highest and lowest daily average direct solar irradiance (W/m^2) on a 22 °C inclination, considered the optimum tilt for the location [30], and the ambient temperature (°C) for the same period.

2.1. Modelling of microgrid system

The mathematical modelling of a microgrid encompasses the development of detailed equations and expressions that capture the physical and operational characteristics of various components. This stage involves modelling the generation sources, including renewable and conventional generators, storage systems, loads, and control strategies that regulate electricity flow within the microgrid. The primary objective is to analyze the microgrid's behaviour under diverse operating conditions, optimize its performance, and ensure stability, reliability, and efficiency.

(a) Grid System Modelling

The grid electricity generation at any time is represented by $P_g(t)$ and modelled as a function of dynamic tariff, capturing the interaction between electricity pricing and the operational decisions of power generation facilities. The instantaneous operational cost $C(P_g,\ t)$,while considering the dynamic tariff $T(t)$ denoting the price at the time (t) is represented by (1):

$$C(P_g, t) = P_g(t).T(t) \tag{1}$$

(b) Solar PV Modelling

The mathematical modelling of solar PV output power generation involves key components like the solar irradiance on the PV panel, the solar cell's efficiency, the impact of temperature, and other environmental factors. The goal of the model is to predict the electrical power output accurately (P_{PV}) from solar PV installation under various conditions. The solar PV power generation is expressed as (2) [26,31]:

$$P_{PV} = \eta.A.G_T \tag{2}$$

where A is the area of the PV panel (m^2), and G_T is the global solar irradiance incident on the PV panels (w/m^2).

Their operating temperature influences the PV cell's performance. The efficiency (η) decreases as the cell temperature increases above the standard test conditions (STC). The temperature effect is accounted for as (3):

$$\eta = \eta_{STC} - \beta\cdot(T_{cell} - 25) \tag{3}$$

Where η_{STC} is the efficiency at STC (25 °C), β is the temperature coefficient of efficiency (%/°C), and T_{cell} is the PV cell temperature in °C. The actual operating temperatures of the PV cell usually vary and are mostly higher. The cell temperature can be estimated using the following formula (4) [26,31]:

$$T_{cell} = T_{amb} + (T_{NOC} - 20)\cdot G_T/800 \tag{4}$$

where T_{amb} is the ambient temperature (°C), and T_{NOC} is the nominal operating cell temperature (°C).

(c) Battery storage Modelling

The BESS operates in bidirectional mode with the charge and discharge modes power expressed as follows (5) [26]:

$$P_b(t) = (1-u)P_{b.chrg}(t) + uP_{b.disch}(t) \tag{5}$$

where, $P_{b.chrg}$ and $P_{b.disch}$ are the battery power during charge and discharge mode and state

$u \in [0,1]$ is specified by the mode of operation as:

$$u = \begin{cases} 1; & discharge\ mode \\ 0; & charge\ mode \end{cases}$$

The charging and discharge power are limited within the stated conditions as follows:

$$\left|P_{b.chrg}\right| \le P_{b.chrg.max}$$

$$\left|P_{b.disch}\right| \le P_{b.disch.max}$$

where, $P_{b.chrg.max}$ and $P_{b.disch.max}$ are the maximum allowed power in the charge and discharge modes.

The battery state of charge (SoC) characterizes the level of charges stored in the battery at any time (t). If $I_c(t)$, $I_d(t)$ are the charge and discharge currents current flowing into and out of the battery, respectively, and η_c, η_d are the losses during the charge and discharge processes. The battery SoC can be estimated from the relation (6):

$$SoC(t) = SoC(t-\Delta t) + \Delta t(\eta_c.I_c(t) - (1/\eta_d).I_d(t)) \tag{6}$$

where $SoC(t-\Delta t)$ represents the SoC at the previous time step and Δt is the time step between successive updates. The common constraint in the battery operation is expressed as:

$$SoC_{min} \le SoC(t) \le SoC_{max}$$

where, SoC_{min} and SoC_{max} are the minimum and maximum allowable battery state of charge specified based on the battery characteristic.

2.2. Problem formulation

The formulated multi-objective energy management optimization is centered around minimizing total energy cost in the microgrid system by limiting the grid purchase while ensuring low battery degradation, as presented in (7):

$$\text{Min } C_{total} = min \sum_{t=0}^{t=24} C_G(t) + C_{b.deg}(t) \tag{7}$$

where C_{total} is the total system generation cost, $C_G(t)$ represents the grid power cost and $C_{b.deg}(t)$ is the battery degrading cost. To achieve minimum operating cost, both the grid power cost under fixed and dynamic tariffs and the battery degradation cost are minimized. The formulated objectives around the two main factors are further explained as follows:

(a) Grid Power Cost Minimization

The grid cost with dynamic time-based tariffs varies according to the time of day and demand level, influencing consumer behaviour and how the utility operates for generations. The idea is to encourage using renewable energy when it's abundant and inexpensive. The objective of this study is to minimize the generation usage cost while meeting the demand and adhering to grid reliability standards (8):

$$C_G(t) = P_g(t).T(t) \tag{8}$$

Table 1
Battery operational modes.

Operational mode	Battery threshold (kWh)	***SoC*** threshold	Charge rate constraint
Mode 1	50–450	$10\% \le SoC \le 90\%$	$\frac{dSoC}{dt} \le -k_{heavy}$
Mode 2	125–375	$25\% \le SoC \le 75\%$	$-k_{mod.max} \le \frac{dSoC}{dt} \le -k_{mod.min}$
Mode 3	200–350	$40\% \le SoC \le 70\%$	$\frac{dSoC}{dt} \le -k_{slow}$

$$min \sum_{i=0}^{i=24} C_G(t)$$

$$\text{subject to } \sum_{i=0}^{i=24} P_{gi}(t, T(t)) = D_i(t, T(t))$$

where, $D(t, T(t))$ is the demand functions and $P_g(t, T(t))$ is the generation function.

(b) Battery Degradation Cost Minimization

The battery degradation minimization is considered one of the multi-objective functions in the study to extend the battery's useful lifespan. It indicates the decline in the performance and capacity of a battery over time due to the charge-discharge cycle, depth of discharge (DoD), temperature, SoC, and charge rate. The battery power cost is modelled as expressed in equation (9) [32–34]:

$$C_{P_b}(t) = P_b(t)C_{bd}(t) \tag{9}$$

where $C_{bd}(t)$ is the battery kWh degradation cost, which is a $f_{cost}(C_N, C_{DoD}, C_T, C_{SoC}, C_{CR})$. The $C_N, C_{DoD}, C_T, C_{SoC}, C_{CR}$ are battery degradation costs due to the number of charge-discharge cycles (N), depth of discharge (DoD), temperature (T), state of charge (SoC), and charge rate (CR) respectively.

$$C_{bd}(t) = C_{cycle}(N, DoD, CR) + C_{calendar}(t, SoC, T) \tag{10}$$

The C_{cycle} and $C_{calendar}$ are cycle and calendar-dependent costs given by (11) and (12), respectively [32–34].

$$C_{cycle} = k.N.(DoD)^{\alpha}.\exp\left(\frac{-E_a}{RT}\right).CR^{\beta} \tag{11}$$

$$C_{calendar} = m.t.exp\left(\frac{-E_a}{RT}\right).SoC^{\gamma} \tag{12}$$

where k and m are combined pre-exponential factors that include unit cost coefficients, then α, β, γ are empirical constants describing the sensitivity of degradation to DoD, CR, and SoC, respectively, and E_a and R are the activation energy and universal gas constant, respectively.

(c) Microgrid Constraints

The formulated multi-objective optimization problem is solved considering equality and non-equality constraints stated as follows:

Equality constraint:

$$P_L(t) = P_{PV}(t) + P_b(t) + P_g(t) \tag{13}$$

Inequality constraint:
SoC constraints: $SoC_{min} \le SoC(t) \le SoC_{max}$.
Battery energy constraint: $E_{b.min} \le E_b \le E_{b.max}$.
Grid power constraint: $P_{g.min} \le P_g \le P_{g.max}$.
Solar PV constraints: $P_{PV.min} \le P_{PV} \le P_{PV.max}$.

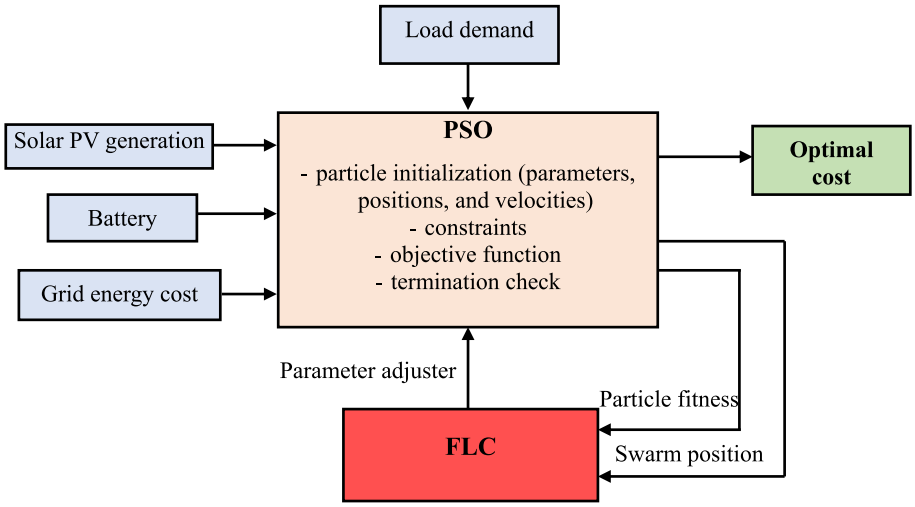

Fig. 4. Proposed FLB-PSO optimization structure.

To limit the battery cycling rate for an improved battery life span while ensuring minimum battery degradation, the battery can be operated in three different modes between the SoC_{min} and SoC_{max}. As presented in Table 1, each operating mode has a different discharge power, with k_{heavy} , $k_{mod.max}$, $k_{mod.min}$ and k_{slow} defined as constants representing heavy, moderate maximum, moderate minimum and slow rate of discharge in their respective mode.

2.3. Multi-objective function optimization

In this work, a multi-objective FLB-PSO algorithm is developed for energy scheduling in microgrid systems to optimize the energy utilization of grid, battery, and solar PV systems. The objective is to minimize the grid power cost and battery degradation cost while taking advantage of solar PV generation. Fig. 4 block diagram presents the structure of the proposed optimization algorithm. The inputs to the FLB-PSO are the hourly instances of solar PV generation, the dynamic grid cost, and the battery power capacity and constraints. The FLB-PSO algorithm fulfills the energy demands from the PV generation augmented by the battery and grid, ensuring optimal battery schedule and grid cost. The FLB-PSO optimization is a variant of PSO where the fuzzy logic controller (FLC) dynamically adjusts the PSO acceleration coefficients parameters c_1 and c_2 based on real-time process feedback and problem characteristics, leading to improved optimization performance and accuracy. The process involves fuzzifying crisp input values into fuzzy sets using membership functions (MF), applying fuzzy logic rules by an inference engine to determine fuzzy outputs, and defuzzification that converts these outputs back into crisp values for adjusting PSO parameters.

A PSO is a computational method that offers the advantages of implementation simplicity, as well as quickly converges to a reasonable solution for complex problems. The solution starts by randomly initializing the positions and velocities of all particles in the swarm (14), (15). The next stage involves the evaluation of each particle using the objective function and keeping track of the best position visited, referred to as the local best p_{best}. The current position of a particle is updated once it has a better fitness value than its previous best, and the best position across the swarm is stored as the global best position g_{best}.

$$Position: x_i = (x_{i1}, x_{i2}, \ldots, x_iD) \tag{14}$$

$$Velocity: v_i = (v_{i1}, v_{i2}, \ldots, v_iD) \tag{15}$$

where x_i is particle position, D is the dimensional search space and v_i is velocity usually initialized randomly.

At each iteration, the particles update their velocities and positions according to the relation (16) followed by a position update with relation (17). The final stage checks for the termination criteria if fulfilled, and if not, then the particle is reevaluated, velocity and position are also updated, and the best position visited by each particle becomes the new local best. In contrast, the best position among all particles becomes the new global best. This cycle continues until the stopping criteria are met.

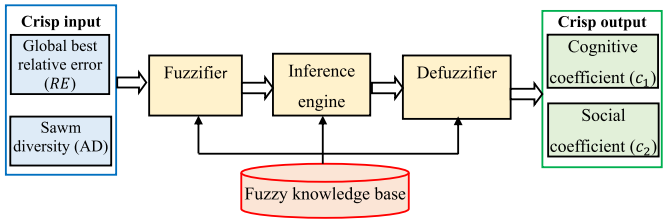

Fig. 5. Fuzzy logic controller with PSO parameters.

$$v_i(t+1) = \omega v_i(t) + c_1 r_1 \left[p_{best(i)} - x_i(t)\right] + c_2 r_2 \left[g_{best(i)} - x_i(t)\right] \tag{16}$$

$$x_i(t+1) = x_i(t) + v_i(t+1) \tag{17}$$

where:

ω is inertial weight that controls the impact of the previous velocity on the current

c_1 and c_2 are cognitive and social acceleration coefficients respectively

r_1 and r_2 are stochastic random numbers between 0 and 1

t is the current iteration

2.3.1. FLB-PSO feedback parameters

The PSO process solution rate of improvement or convergence relative error, and the swarm particle diversity parameters served as feedback input into the Fuzzy logic controller. The feedback mechanisms monitor the algorithm performance, and the FLC uses the measured values to adjust the PSO parameters accordingly. The process stages presented in Fig. 5 start by crisping the input feedback parameter, then to the fuzzy inference system and crisp outputs. The acceleration coefficients, including the cognitive (c_1) and social (c_2) factors are adjusted based on the global best convergence relative error (RE) and swarm diversity average distance (AD) based on the FLC's predefined rules. The c_1 encourages the exploitation of the search space based on the particle's experience. A higher value means that particles are more influenced by their memory, potentially leading to faster convergence while increasing

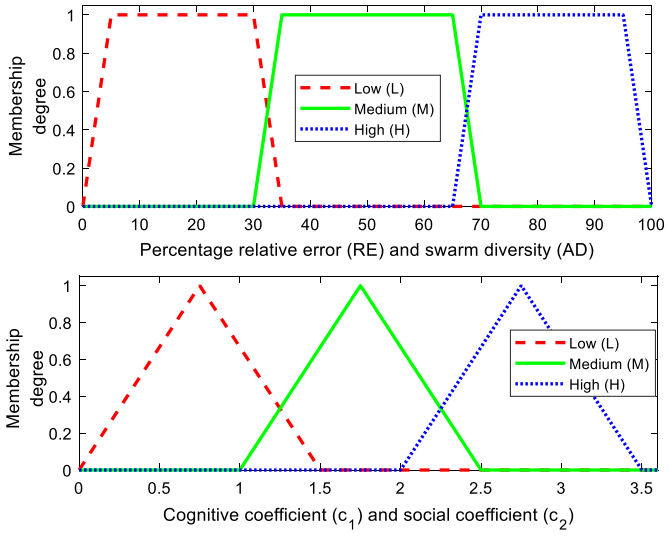

Fig. 6. Fuzzy input and output membership functions.

the risk of getting stuck in local optima. c_2 facilitates the utilization of the swarm's collective knowledge, promoting convergence towards promising areas of the search space or the global best position found by the swarm. Like the cognitive coefficient, a higher value accelerates convergence, but can also lead to premature convergence if too high.

The metric for evaluating the convergence rate of PSO optimization algorithms is the convergence speed, measured using fitness value progression by tracking the progression of the best fitness value achieved by the swarm over generations or iterations. In this work, the rate at which the algorithm converges was calculated by analyzing the change in fitness values over successive iterations as a relative error (*RE*). The *RE* was computed using the difference between consecutive fitness values as expressed in (18). A positive relative error suggests particle divergence, while a negative relative error indicates convergence progress.

$$RE = \frac{Fitness_{current} - Fintness_{previous}}{Fitness_{current}} \tag{18}$$

The PSO diversity is measured by population spread, calculating the dispersion of particles in the search space. Metrics such as standard deviation, variance, and entropy of particle positions, along with fitness gradient and fitness variance, are used to quantify swarm diversity. In this work, the average distance (*AD*) metric was used to measure the swam diversity as feedback. It involves computing pairwise distances between particles and finding the average to indicate their spread out in the search space. The Euclidean distance to every other particle in the swarm is computed for each particle. In a two-dimensional space, the Euclidean distance between two particles with coordinates (x_1, y_2) and (x_2, y_2) can be computed from (19):

$$Euclidean\ distance = \sqrt[2]{(x_2 - x_1)^2 + (y_2 - y_1)^2} \tag{19}$$

The *AD* is then computed across all pairs of particles as the ratio of the sum of distances to the number of pairs in the swarm, representing the separation between particles in the search space. A larger average distance between particles indicates a more diverse swarm. Conversely, a smaller average distance suggests that particles are clustered closely, potentially leading to a lack of exploration and diversity in the swarm.

2.3.2. Fuzzy logic membership function

The PSO signals are used as a control parameter mechanism to determine the direction of c_1 and c_2 adjustment. If the swarm is too dispersed, indicating excessive exploration, then the Fuzzy algorithm increases c_2 to enhance social learning and decrease c_1 to reduce the reliance on individual knowledge. If the swarm is quickly converging, indicating less exploration, the algorithm decreases c_2 to limit social learning and increase c_1 to improve the individual knowledge exploitation. The magnitude of adjustment establishes how significantly the parameters are modified. The default c_1 and c_2 values were set to 2, and to prevent excessive changes that could destabilize the search process, the adjustment magnitude was bounded to a step change of 0.2 or 10 % change of the nominal. The inputs and outputs of MF are categorized into spectrums labelled low (*L*), medium (*M*), and high (*H*), quantify the degree to which they belong. The MF for the input parameters improvement rate of global best is computed as *RE* (18) and average swarm distance *AD* computed from (19) were defined for adapting the PSO output parameters c_1 and c_2.

Table 2
Proposed Fuzzy inference rule for the FLB-PSO.

Improvement rate of global best, *RE*	Swarm Diversity, *AD*	Adjustment of cognitive coefficient (c_1) and social coefficient (c_2)
Low, *L*	Low, *L*	c_1 increase, c_2 is maintain
	Medium, *M*	c_1 maintain, c_2 is maintain
	High, *H*	c_1 maintain, c_2 is decrease
Medium, *M*	Low, *L*	c_1 maintain, c_2 is maintain
	Medium, *M*	c_1 maintain, c_2 is maintain
	High, *H*	c_1 maintain, c_2 is decrease
High, *H*	Low, *L*	c_1 decrease, c_2 is maintain
	Medium, *M*	c_1 decrease, c_2 is maintain
	High, *H*	c_1 decrease, c_2 is decrease

MF plays a crucial role in quantifying the linguistic variables representing inputs and outputs when designing the FLC to adapt the PSO acceleration coefficients. For the input parameters, the *RE* and *AD* are captured with the spectrum of *L*, *M*, and *H* classes. At the input, a trapezoidal MF with appropriate ranges is defined for the *RE* and *AD* parameters, ranging from 0 % to 100 % as presented in Fig. 6. When the *AD*, diversity value is smaller, ranging from 0 % to 35 % relative to the initial average distance, indicating low particle diversity; the MF is defined with the *L* class. The *M* class corresponds to moderate diversity from 30 % to 70 %, while the *H* class is defined for high diversity from 65 % to 100 %. Similarly, *RE* convergence values of 0 %–35 %, 30 %–70 %, and 65 %–100 % indicate high, moderate, and low convergence, respectively, which are classified as *H*, *M*, and *L* classes. For the output parameters, the coefficients c_1 and c_2 factors, triangular MFs were selected as presented in Fig. 6. This also spans *L*, *M*, and *H* classes, ranging from 0 to 3.5, reflecting the desired adjustment for the PSO acceleration coefficient parameters. The *L* range values cover 0 to 1.5, within which the coefficients step decrease, while the *M* values range from 1 to 2.5, for which the coefficients are maintained, and 2 to 3.5 for *H* value for which the coefficients are increased. The choice of trapezoidal MFs for input parameters and triangular MFs for output parameters is motivated by the need for clear, interpretable boundaries for input classes and precise adjustments for output coefficients, ensuring effective adaptation of the PSO algorithm to varying conditions.

2.3.3. Rule formulation for inference engine

The designed FLC takes multiple inputs, the global best improvement rate inputs, and swarm diversity to adjust PSO parameters based on the defined fuzzy rules. This approach allows a nuanced adaptation of a fuzzy inference system with the appropriate MFs and regulations. The rules were crafted by prior experience and empirical observations to adjust the PSO algorithm parameters dynamically. The FLC continuously adjusts the c_1 and c_2 to achieve balanced exploration and exploitation. Ultimately, the proposed hybrid FLB-PSO approach allows the adaptive capabilities, enabling it to respond flexibly to changes in the optimization landscape and improve its convergence speed and solution quality across various optimization tasks.

The developed fuzzy *IF* − *AND* − *THEN* rules describe how the PSO parameters are adjusted based on the inputs. The rules form the core of the FLC, guiding the system response to changes in the optimization

Table 3
Hybrid energy system components.

Components	Rating
Solar PV array	500 kW, 500V
BESS capacity	500 kWh
BESS efficiency	95 %
BESS SoC minimum	20 %
BESS SoC maximum	80 %
BESS degradation cost	$0.04
DC-DC boost converter	500 kVA, 600 dc
Bidirectional DC-DC converter	250 kVA, 600 dc
Bidirectional inverter	1 MVA, 11 kV
Grid buying/Selling (off-peak)	$0.18
Grid buying/Selling (peak)	$0.25

process. The summary of the adaptation fuzzy rules for step adjusting the output parameters c_1 and c_2 factors of the PSO algorithm independently based on the *RE* and *AD* values as inputs are presented in Table 2.

The rules ensure that each acceleration factor can be increased, maintained, or decreased separately depending on the specific conditions. For example, *IF* improvement rate of global best *RE* is Low *AND* swarm diversity *AD* is Low *THEN* factor c_1 increased while c_2 is maintained. That is if the solution *RE* is low, and the *AD* is also low, indicating slow progress and limited exploration, then the c_1 is increased to encourage more exploration. Meanwhile, the c_2 remains unchanged to maintain the existing level of collaboration among particles. In the same manner, *IF RE* is Low *AND AD* is High *THEN* c_1 is maintained while c_2 is decreased. This can be interpreted as if the improvement rate of the global best solution is low and the swarm diversity is high, indicating slow progress but high exploration, then the c_1 remains unchanged to maintain the current level of exploration, while the c_2 is decreased to reduce collaboration and encourage more individual exploration. The subsequent rules follow a similar logic, adjusting c_1 and c_2 based on the combination *RE* and *AD* to balance exploration and exploitation in the PSO algorithm, ensuring adaptability to different optimization landscapes and problem characteristics.

2.3.4. Defuzzification

The defuzzification stage of the FLC involves obtaining a crisp number from the output of the aggregated fuzzy set. It transferred the fuzzy inference results into a crisp output. Several methods have been reported in the literature, including the center of gravity or area (COG), mean of maximum (MOM), first of maximum (FOM), mean of maxima (MeOM) methods, and others [35]. Among these methods, the centroid method, largely favoured due to its accuracy and simplicity of implementation, is selected in this work. The COG method finds the center of mass of the fuzzy output set, resulting in a precise parameter adjustment value. For the discrete MF, the defuzzified value denoted as centroid x^*, with COG is defined as (20) [35]:

$$Centroid, x^* = \frac{\sum_{i=1}^{n} x_i \mu(x_i)}{\sum_{i=1}^{n} \mu(x_i)} \tag{20}$$

Where x_i denotes the sample element, $\mu(x_i)$ is the MF, and n is the number of elements in the sample.

2.4. System specifications and simulation

The hybrid energy system test bed comprises solar PV interconnected to the utility grid through a DC/AC inverter. The PV arrays are connected in series and parallel strings to produce an 800 kW/500V system, which is then connected to a DC bus via a DC-DC boost converter. The DC-DC converter boosts and stabilizes the 500V voltage to serve the inverter. The battery energy storage system is a 500 kWh, 1250 Ah, 400 V unit connected via a bidirectional DC-DC boost converter. The AC bus

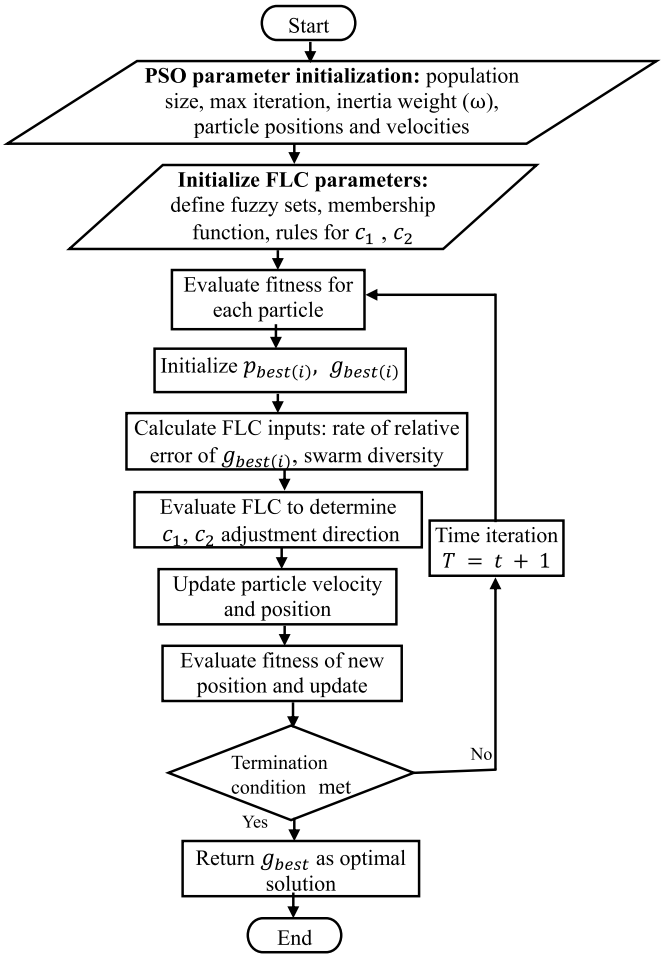

Fig. 7. FLB-PSO optimization algorithm.

operates at 11 kV, and the inverter that transfers energy from the battery and solar PV to the AC bus is rated at 1 MW. The component ratings of the simulation test system are summarized in Table 3.

The microgrid system components were first simulated in the MATLAB/Simulink environment to obtain an accurate solar PV generation. The battery was modelled as a lithium-ion battery with a 500 kWh capacity, as specified in Table 3. The grid system was modelled as a three-phase voltage source in series with an RL branch, and the loads were implemented with a three-phase parallel RLC circuit. The solar PV was constructed with 8 units of 100 kW PV arrays, each comprising 64 parallel string SunPower SPR-315E-WHT-D modules with 5 series-connected modules per string to meet the current and voltage demand, respectively. To achieve precise energy generation from the solar PV over 24 h, the solar irradiance and temperature at the considered location were fed into the PV array. Additionally, each PV was attached to a maximum power point tracker (MPPT) controller based on the perturb and observe (P & O) method. The MPPT ensures maximum power harvesting from the solar PV array by continuously adjusting the operating point, observing the power output, and perturbing the operating voltage to meet the reference voltage corresponding to the maximum power point.

The FLB-PSO EMS algorithm was implemented using a MATLAB m-file script that takes inputs such as solar PV power, load demand, battery capacity, battery efficiency, and grid cost. The algorithm was executed on an Intel Core i3-3217U CPU @ 1.80 GHz with 8 GB of RAM, following Fig. 7 flow chart. It performs real-time control actions to adjust energy flow based on current supply and demand conditions and updated optimization results. The algorithm determines optimal energy flows

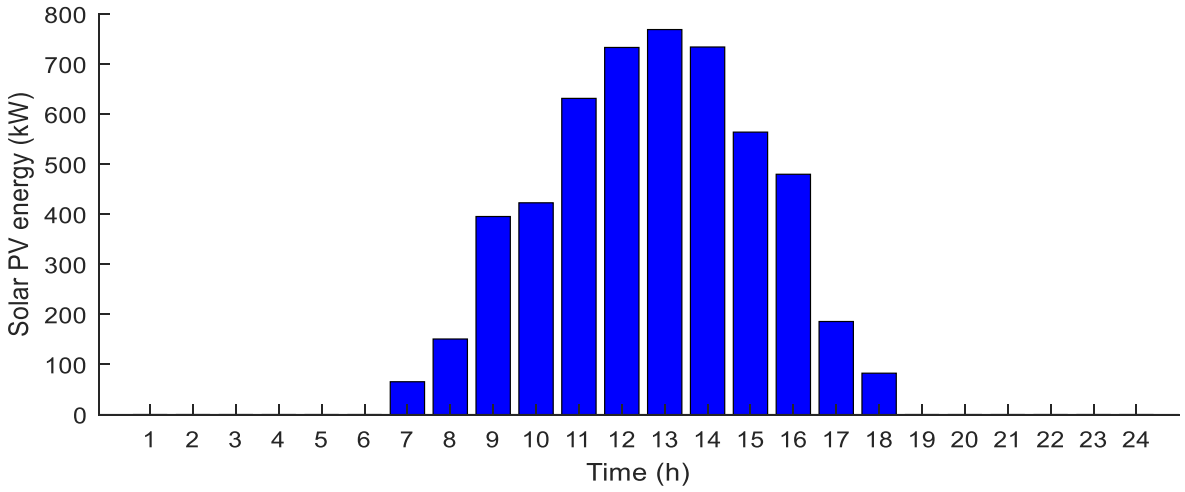

Fig. 8. Daily average solar PV energy generation.

Table 4
Optimal parameter values in 10:00 h.

Optimal values	80 % battery ***SoC*** capacity	30 % battery ***SoC*** capacity	50 % battery ***SoC*** capacity
Grid power (kW)	343.6617	330.3313	269.1307
Battery power (kW)	30.5478	43.8787	105.0793
Objective function values			
Grid power purchase/ sales cost ($)	61.8592	59.4596	48.4435
Battery degradation cost ($)	1.2219	1.7552	4.2032

Table 5
Optimal parameter values in 21:00 h.

Optimal values	80 % battery ***SoC*** capacity	30 % battery ***SoC*** capacity	50 % battery ***SoC*** capacity
Grid power (kW)	763.4944	1031.8256	889.9621
Battery power (kW)	193.0756	75.2556	25.4679
Objective function values			
Grid power purchase/sales cost ($)	137.4289	185.7286	160.1932
Battery degradation cost ($)	7.7230	3.0102	1.0187

Table 6
Optimal parameter values in 24 h period.

Optimal values	80 % battery ***SoC*** capacity	30 % battery ***SoC*** capacity	50 % battery ***SoC*** capacity
Grid power (kW)	10622.3787	10938.6979	10750.4115
Battery power (kW)	2368.2039	1004.0553	1248.3521
Objective function values			
Grid power purchase/sales cost ($)	1912.0282	1968.9656	1935.0741
Battery degradation cost ($)	94.7282	40.1622	49.9341

between energy sources and the load hourly over a 24-h period, aiming to minimize total operational costs while meeting energy demand and system constraints. The PSO and FLC parameters, including fuzzy sets, membership functions, and rules, are set at the start. The initial fitness of each particle is evaluated to set the $p_{best(i)}$ and $g_{best(i)}$ positions. The algorithm enters a loop until the maximum number of iterations is reached or convergence criteria are met. Within the loop, FLC inputs are used to calculate new values for PSO coefficients c_1 , and c_2, which is used to update particle velocities and positions. The algorithm terminates when the maximum number of iterations is reached, or an acceptable level of convergence is achieved, with the final optimal solution corresponding to the g_{best} particle's position.

3. Results and discussion

This section presents the performance evaluation of the proposed FLB-PSO algorithm for a hybrid EMS. The algorithm was implemented in a MATLAB environment within a grid-connected microgrid system with solar PV panels and battery energy storage system energy sources. In the simulation, the PV energy source generates sufficient power to meet a significant portion of the demand during the day, and any excess energy is used to charge the batteries. Fig. 8 presents the monthly average daily solar PV energy generation at the study location, with peak generation occurring at 13:00 h. The daily load demand varies between 458 kWh and 957 kWh, with peak demands occurring in the early morning and nighttime hours, as depicted in Fig. 2. The study location's current fixed grid electricity tariff stands at ₦225, equivalent to $0.18. This is the same for off-peak periods under dynamic tariffs. The peak dynamic tariff spanning 6:00 h to 9:00 h and the 18:00 h to 22:00 h has an increase of 40 %, amounting to $0.25, away from the nominal off-peak tariff of $0.18.

4. FLB-PSO EMS performance under fixed grid tariff

The FLB-PSO's performance on the energy mix for load operation at optimal daily cost was evaluated under both fixed and dynamic grid tariffs. The first test scenario considered a fixed grid power tariff when solar PV generation was insufficient and the battery SoC threshold could not meet the load demand. The results of the FLB-PSO EMS algorithm's hourly operating cost for two selected periods, 10:00 and 21:00 h, are presented in Tables 4 and 5, respectively.

As one of the main objectives of this study, battery degradation is a critical factor, and the test results for three different operational modes are included in Table 4. These results indicate diverse grid power purchase and battery degradation costs. The battery's first operational mode allows an 80 % battery SoC range, while the second mode allows a 30 % battery SoC range. The optimal Pareto solution was obtained in the third mode, which allows a 50 % battery SoC range, resulting in the minimum daily energy cost by balancing grid purchase with battery degradation costs. Balancing grid power purchases and battery degradation is crucial for cost reduction and extending the battery lifespan,

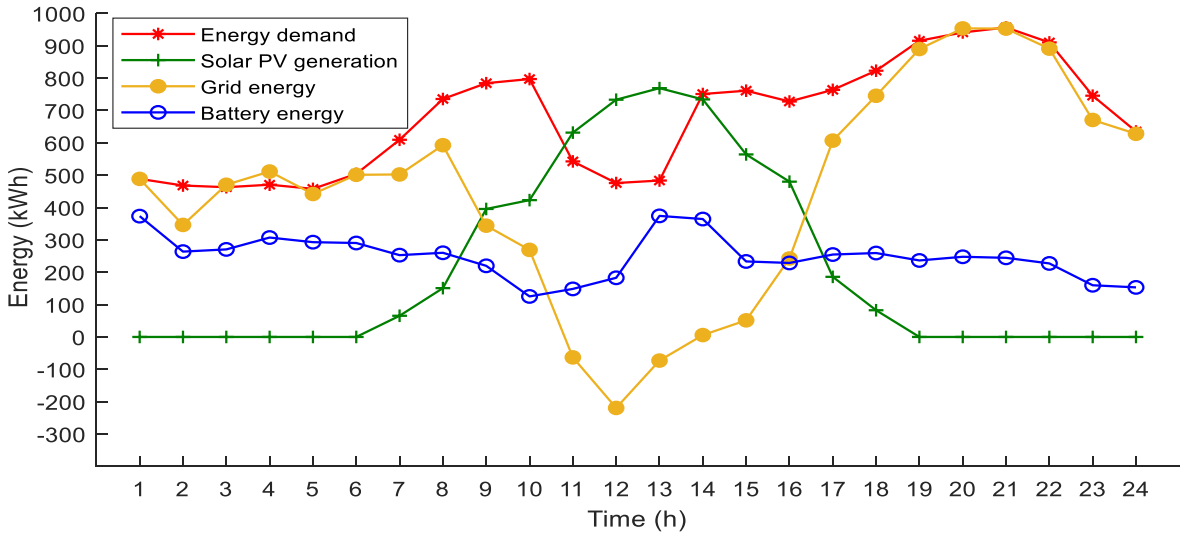

Fig. 9. Energy profile of demand in 24 h.

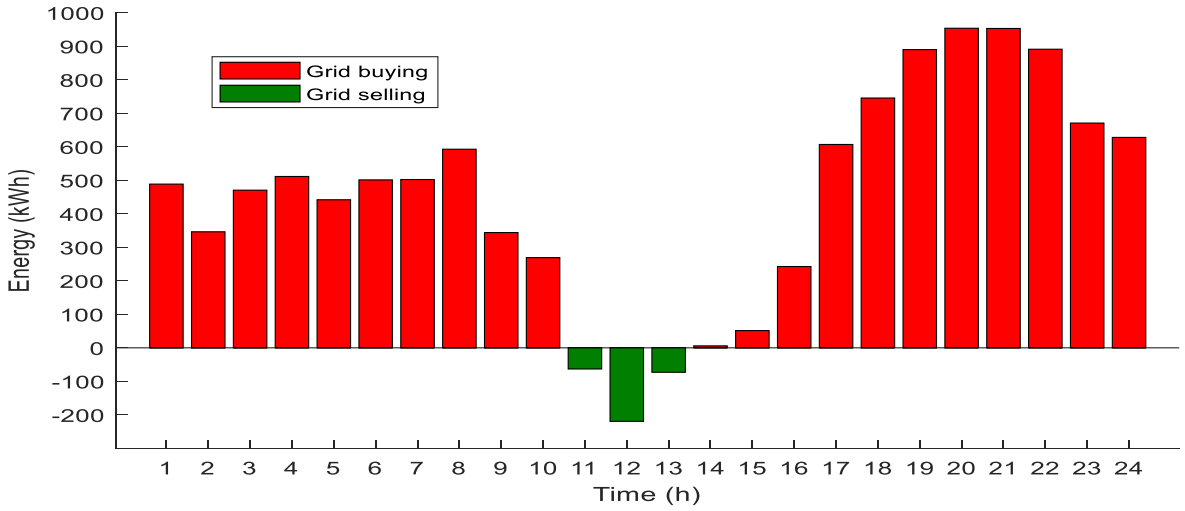

Fig. 10. Grid energy buying/selling in 24 h period.

thereby reducing replacement costs.

The results of the 24-h daily energy operational costs with the FLB-PSO EMS algorithm are presented in Table 6 for the three battery operational modes. In Mode 1, with 80 % battery SoC capacity, grid purchase is limited to $1912.03, which incurs a higher battery degradation cost of $94.73. Mode 2, with 30 % SOC capacity, reduces the battery degradation cost to $40.16, but the grid purchase cost increases to $1968.97. Mode 3, with 50 % battery SoC capacity, balances the grid purchases and battery degradation costs at $1935.07 and $49.93, respectively. This results in a total daily operational cost of $1985.01, compared to $2006.76 and $2009.13 for Modes 1 and 2, respectively. Mode 3 demonstrated the optimal Pareto solution by achieving the dual objectives of minimizing both grid purchase and battery degradation costs, resulting in the lowest daily energy operating cost.

The microgrid energy profile is depicted in Fig. 9, illustrating the load demand, solar PV generation, utility grid power, and battery charge/discharge over 24 h. The combined energy production from renewable power generation, battery discharge, and energy imported from the utility grid meet the energy demand. During peak daytime generation, solar PV significantly supplies the load demand, with any excess energy either stored in the battery or sold to the grid, depending on the battery SoC. Fig. 9 shows that the battery SoC is maintained at a high level between 12:00 and 15:00 h since renewable generations meet most energy demands. Between 12:00 and 14:00 h, excess PV generation is used to charge the battery, while the remaining power is sold to the grid during the same period.

Fig. 10 presents the main grid energy purchases and sales over a 24-h period. Energy purchases vary throughout the day but are highest at nighttime during peak energy demand when only the battery is available for supplementary supply without renewable energy generation. Grid power sales occur at 11:00, 12:00, and 13:00 h when there is excess solar PV generation. Fig. 11 (a) shows the battery's intermittent charging and discharging over 24 h, with most charging occurring during hours of high renewable generation. Fig. 11 (b) depicts the battery SoC profile within the constraints set at a 25 % SoC minimum and a maximum of 75 % SoC for the optimization process. The 50 % SoC battery capacity delivers the optimal operational cost and efficiency, ensuring extended battery lifespan while meeting the daily energy demand.

Fig. 12 (a) and (b) present the battery degradation and utility grid costs under a fixed tariff for the proposed FLB-PSO EMS and conventional PSO EMS. The battery degradation cost, representing the cost associated with the decline in battery performance and capacity over time due to charge-discharge cycles, was set to $0.04 per kWh for utility-scale battery storage in this study, as contained in recent literature

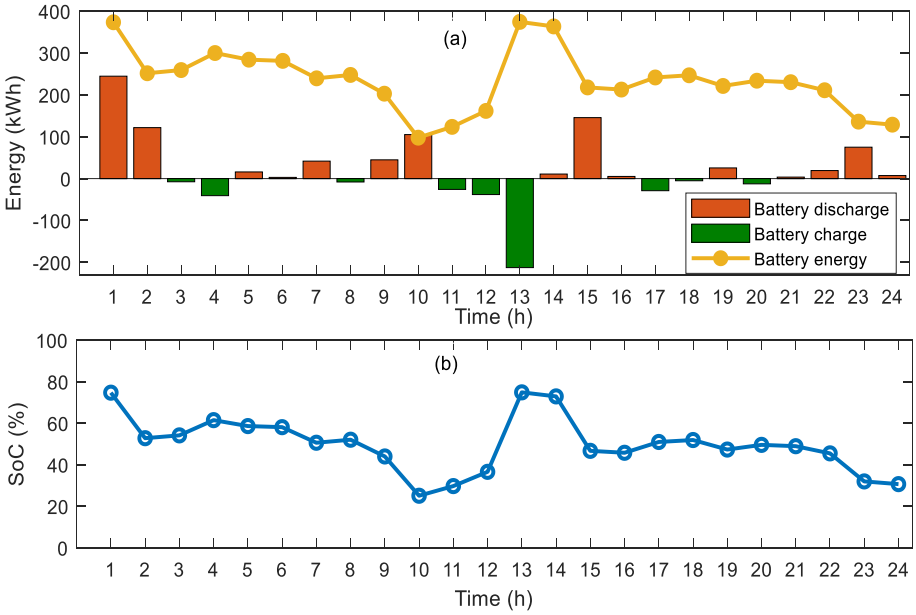

Fig. 11. Battery charge/discharge (a) and SoC profile (b).

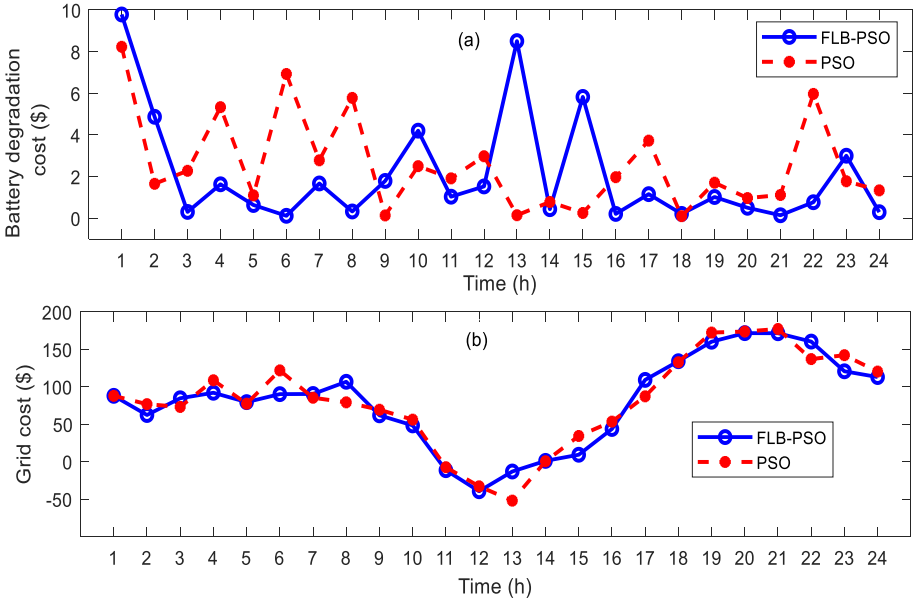

Fig. 12. EMS battery degradation cost (a) and grid cost (b) under fixed tariff.

findings [36]. In Fig. 12 (a), the FLB-PSO battery degradation cost was lower during most operational hours in the morning and evening but significantly higher in the afternoon when renewable generation peaks and charges the battery. The battery profile in Fig. 11 indicates that the FLB-PSO EMS charges the battery more during the hours of 12:00 to 15:00, when renewable generation is abundant, and moderately supplies this energy to the load throughout the day, thereby avoiding the higher degradation costs seen with PSO in the morning and evening hours. This smoothing of battery degradation costs by FLB-PSO demonstrates its superiority in optimizing the EMS solution, ultimately reducing grid purchase and the total daily energy cost.

Fig. 12 (b) show that FLB-PSO prioritizes charging the battery during peak renewable generation periods rather than selling excess energy to the grid, as opposed to the PSO, which sells more and subsequently buys more energy later in the day. This strategy results in a reduction in grid costs between 15:00 and 24:00 h. Specifically, FLB-PSO grid purchases are lower during 15:00, 16:00, 19:00, 20:00, 21:00, 23:00, and 24:00 h, compared to the PSO, which shows lower grid purchases only at 17:00 and 22:00 h.

The convergence plot under a fixed grid tariff for the FLB-PSO and PSO algorithms are presented in Fig. 13. The plots show that the PSO converges after 40 iterations, while the FLB-PSO rapidly converges after just 3 iterations. The proposed methods achieved fast convergence speed by balancing exploration and exploitation during the optimization. The achieved convergence speed surpasses that of some state-of-the-art methods, as reported in Ref. [37], Çetınbaş et al. [38], Zhao et al. [39]. These studies exhibit convergence within 10–50 iterations when using various advanced algorithms to optimize hybrid energy systems. Initially, the PSO starts at $2290 and converges to $2221.10 after 40 iterations. In contrast, despite starting from a significantly larger initial value of $200,000, the FLB-PSO converges to $1985.01 after only 3 iterations. The quick convergence and superior solution of the FLB-PSO

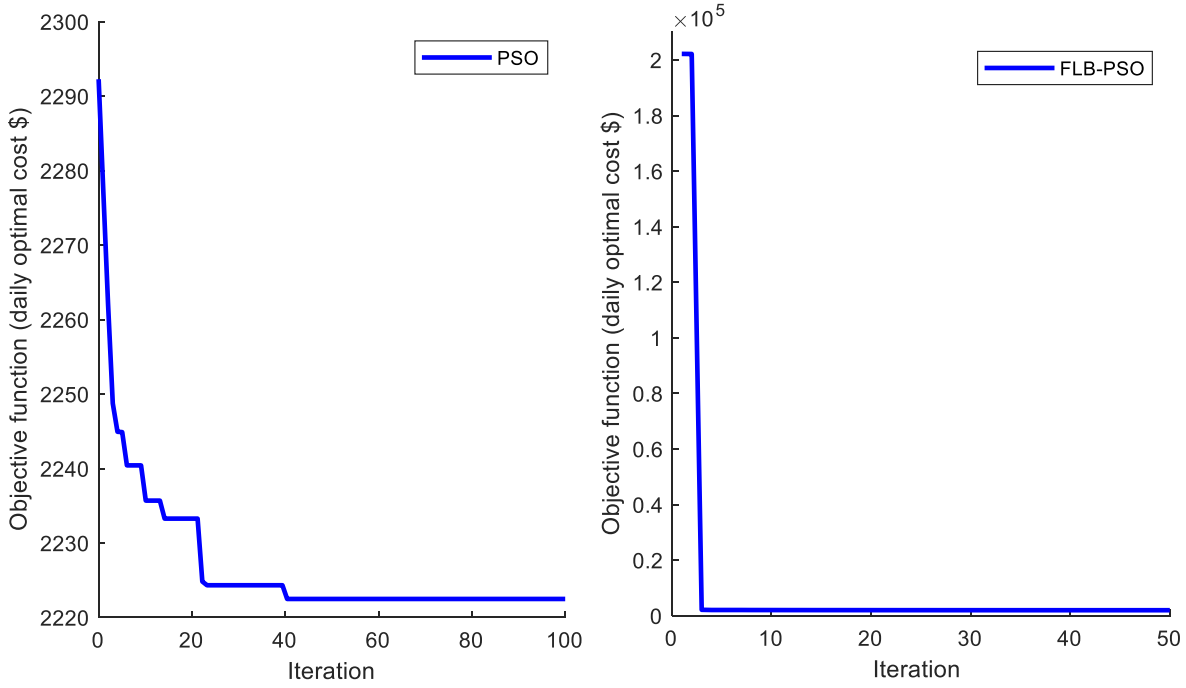

Fig. 13. Convergence plot under fixed grid tariff.

Table 7
Optimal cost comparison of the proposed EMS under fixed tariff.

Optimal values	Proposed FLB-PSO EMS	Conventional PSO EMS
Grid power purchase cost ($)	1935.0741	2159.670605
Battery degradation cost ($)	49.9341	61.42916699
Total	1985.0082	2221.0998

Table 8
Optimal parameter values in the 02:00 h.

Optimal values	80 % battery ***SoC*** capacity	30 % battery ***SoC*** capacity	50 % battery ***SoC*** capacity
Grid power (kW)	150.4364	435.2540	467.9900
Battery power (kW)	317.5636	32.7460	0.0070
Objective function values			
Grid power purchase/ sales cost ($)	27.07856	78.3457	84.2382
Battery degradation cost ($)	12.7025	1.3098	0.0004

Table 9
Optimal parameter values in 15:00 h.

Optimal values	80 % battery ***SoC*** capacity	30 % battery ***SoC*** capacity	50 % battery ***SoC*** capacity
Grid power (kW)	25.6347	121.2739	171.8056
Battery power (kW)	171.3553	75.7161	25.1844
Objective function values			
Grid power purchase/ sales cost ($)	4.6143	21.8293	30.9250
Battery degradation cost ($)	6.8542	3.0286	1.0074

indicate that the proposed optimization algorithm is highly effective, well-adapted, and capable of robust performance across a wide range of initial conditions. This performance confirms its exploration capability in searching the solution space. The daily optimized energy operational cost of $1985.01 for FLB-PSO in Table 7, compared to $2221.10 for PSO, demonstrates its excellent exploitation by effectively refining the solution towards an improved optimal outcome. The cost difference shows that the FLB-PSO saves $236.09, approximately 11 %, on daily energy costs. These traits of robustness and efficiency are highly desirable in real-time EMS and many practical optimization scenarios.

Table 10
Optimal parameter values in 24 h period.

Optimal values	80 % battery ***SoC*** capacity	30 % battery ***SoC*** capacity	50 % battery ***SoC*** capacity
Grid power (kW)	10711.0280	10871.5142	10717.2909
Battery power (kW)	2360.2494	2412.8403	1616.4218
Objective function values			
Grid power purchase/sales cost ($)	2288.1535	2412.8403	2359.1965
Battery degradation cost ($)	91.5261	53.0968	64.6569

4.1. FLB-PSO EMS performance under dynamic grid tariff

The second test case scenario considered a dynamic grid tariff for purchasing utility power while maximizing the use of solar PV generation to meet daytime load demand and using excess energy to charge the battery. Tables 8 and 9 present the hourly operating costs of the FLB-PSO EMS algorithm for two selected periods, 02:00 and 15:00 h, respectively, while Table 10 shows the 24-h costs.

In Table 10, battery mode 3, which denotes 50 % battery capacity, balances the daily grid purchase and battery degradation costs at $2359.20 and $64.66, respectively. This results in a total daily operational cost of $2423.85, compared to $2379.68 for mode 1 and $2465.94 for mode 2. The advantage of mode 3 lies in balancing the multi-objective functions of minimizing grid purchases and battery degradation costs rather than relying heavily on the battery, as in mode 1, which would lead to rapid battery degradation and high replacement costs.

The microgrid energy profile under dynamic tariff is presented in Fig. 14, illustrating the load demand, solar PV generation, utility grid

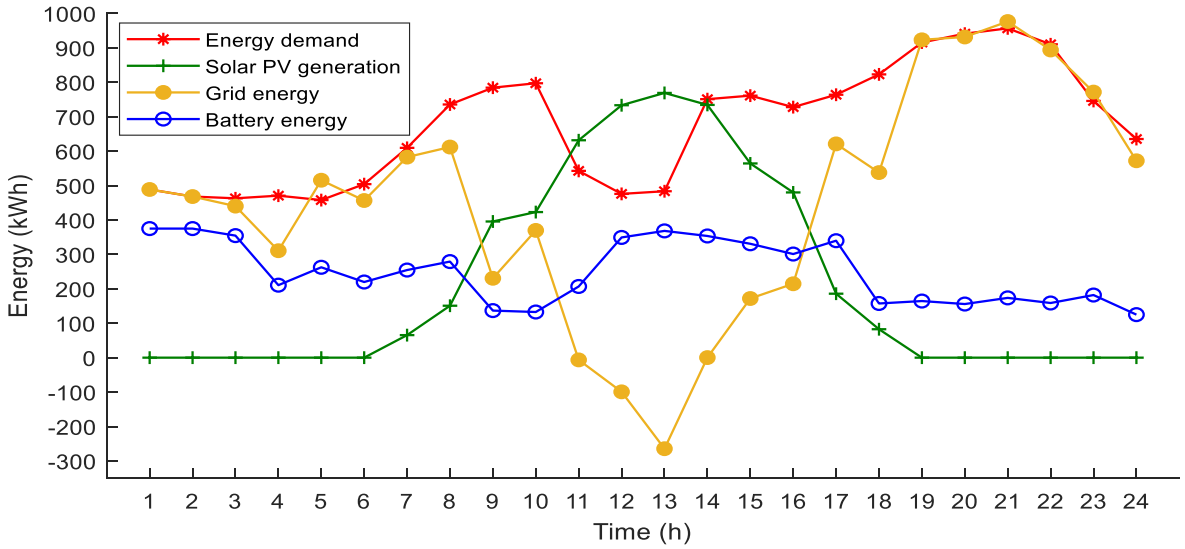

Fig. 14. Energy profile of demand in 24 h.

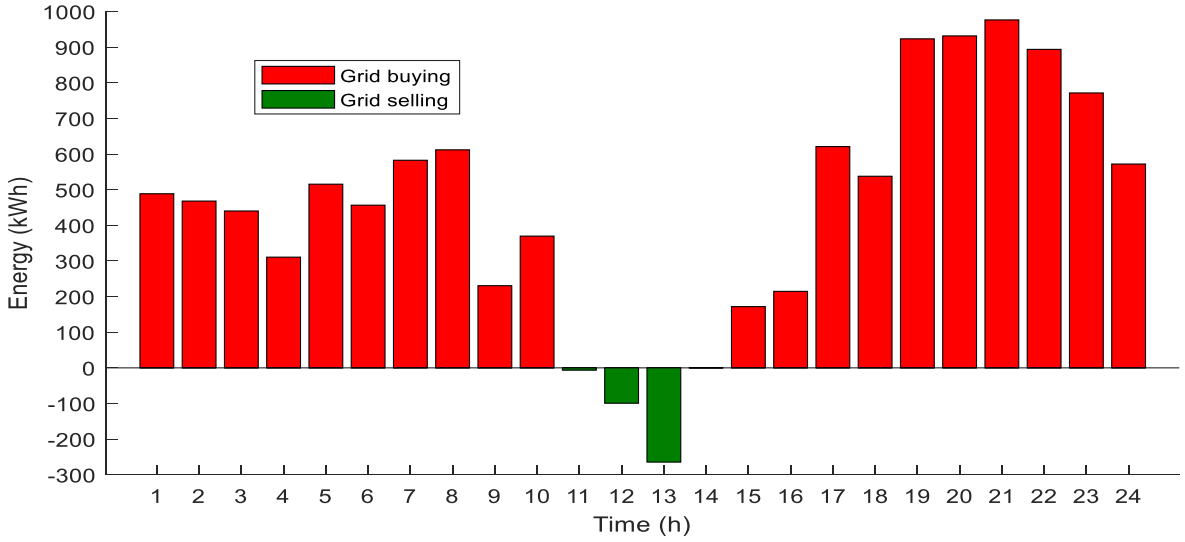

Fig. 15. Grid energy buying/selling in 24 h period.

power, and battery charge/discharge over 24 h. During peak daytime generation, the load demand is primarily met by solar PV energy, with any excess energy either stored in the battery or sold to the grid, depending on the battery SoC. From 12:00 to 15:00 h, the battery SoC remains relatively stable at a high charge level during peak renewable generation, while the surplus power is sold to the grid during this period.

Fig. 15 presents the main grid energy purchases and sales over a 24-h period. Energy purchases vary throughout the day, with higher purchases occurring at night during peak energy demand when there is no renewable energy generation, and the battery provides a complementary supply. As shown in the figure, grid power sales occur during 11:00, 12:00, and 13:00 h when there is excess solar PV generation. Fig. 16 (a) depicts the 24-h intermittent charging and discharging of the battery, with most charging occurring during the high renewable generation hours between 11:00 and 14:00. The figure also reveals the battery's complementary actions during peak tariff hours, with increased discharging between 07:00 and 10:00, thereby reducing grid purchases. Fig. 16 (b) shows the battery SoC profile operating within the specified minimum SoC of 25 % and maximum SoC of 75 %, as specified constraints for the optimization problem to ensure extended battery lifespan.

Fig. 17 (a) and (b) present the battery degradation and grid costs under dynamic tariff for the proposed FLB-PSO and conventional PSO EMS. In Fig. 17 (a), the FLB-PSO battery degradation cost is observed to be lower for most operational hours and significantly higher during peak tariff hours when the battery supplements grid purchases to reduce hourly operating costs. Fig. 16 revealed that the FLB-PSO prioritizes charging the battery during peak renewable generation periods rather than selling excess energy to the grid. This is evident in the grid cost depicted in Fig. 17 (b), particularly between 11:00 and 13:00 h, compared to PSO, which sells more to the grid. This strategy significantly reduces grid purchases during the peak tariff period of 18:00 and 19:00 h, lowering daily operational costs.

The convergence under dynamic grid tariff for the proposed FLB-PSO was attained after 3 iterations compared to the PSO algorithms that converged after 40 iterations. The PSO starts the search at $2745 and converges to $2661.08 after 40 iterations. In contrast, the FLB-PSO quickly converges to $2423.85 after three iterations despite starting from a significantly higher initial value of $200,000. The quick convergence and superior solution of the FLB-PSO under dynamic tariff conditions also indicate the effectiveness, adaptive tuning capability, and robust performance of the proposed optimization algorithm. This

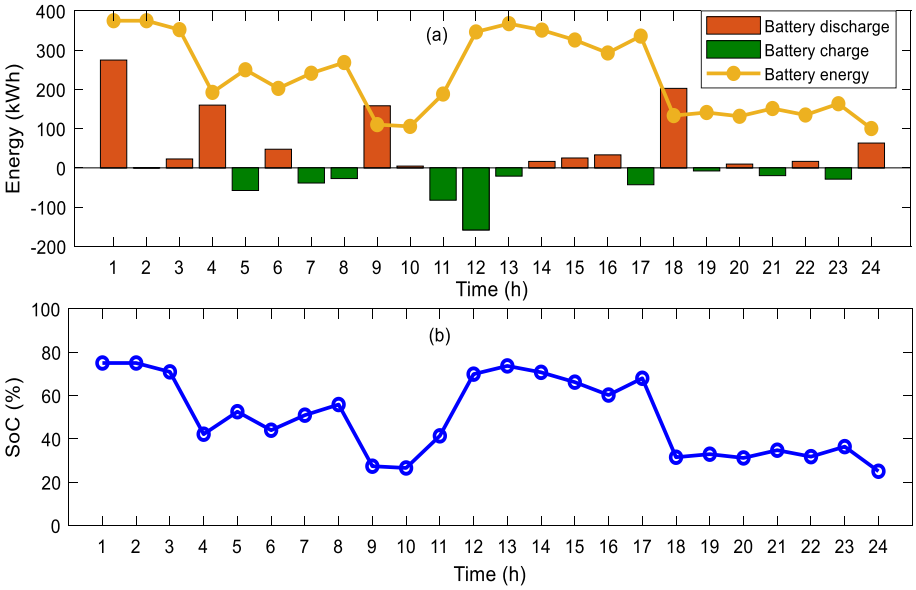

Fig. 16. Battery charge/discharge (a) and SoC profile (b).

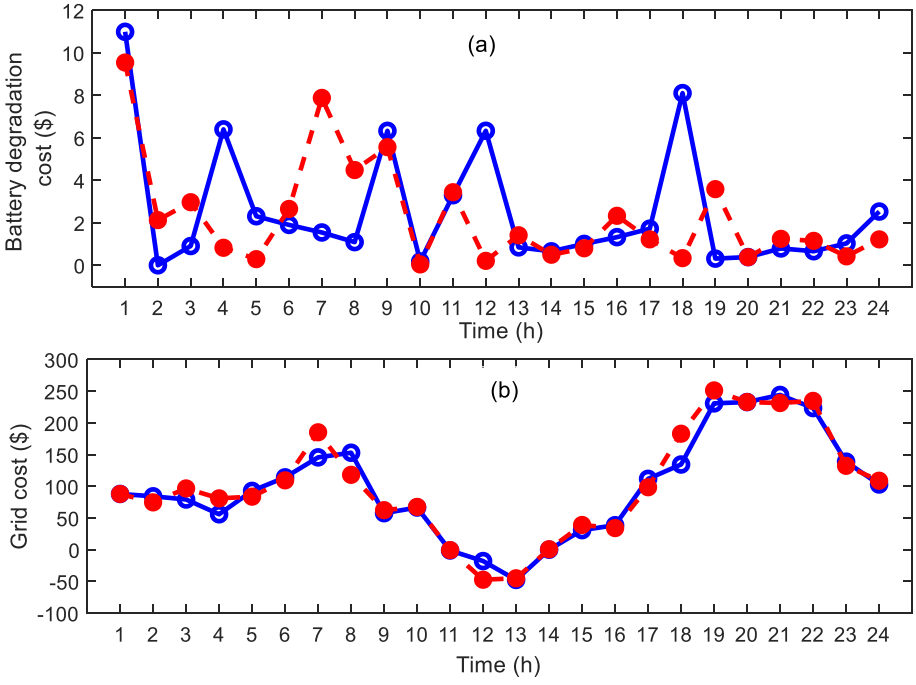

Fig. 17. EMS battery degradation cost (a) and grid cost (b) under dynamic tariff.

Table 11
Optimal cost comparison of the proposed EMS under dynamic tariff.

Optimal values	Proposed FLB-PSO EMS	Conventional PSO EMS
Grid power purchase cost ($)	2359.1965	2606.4702
Battery degradation cost ($)	64.6569	54.6120
Total	2423.8534	2661.0823

result confirms its ability to explore a more widespread solution space and achieve rapid convergence. The daily optimized energy operational cost in Table 11 shows that the FLB-PSO results save $237.23 compared to PSO, representing a 9 % reduction in daily energy costs.

The proposed FLB-PSO EMS algorithm was tested under fluctuating weather conditions to further demonstrate its robustness and efficiency. The energy profile in Fig. 18 depicts the load demand, solar PV generation, utility grid power, and battery charge/discharge over 24 h to demonstrate its robustness and performance in more realistic scenarios. Solar power generation drastically decreased between 10:00 and 12:00 h, affecting the available diverse energy mix. However, the EMS algorithm effectively responded by importing more grids to balance the energy needs. The EMS algorithm prioritized battery charging as a quick response to an increase in solar PV generation from 13:00 h, showing its effectiveness.

5. Conclusion

This study presents an efficient energy management strategy using

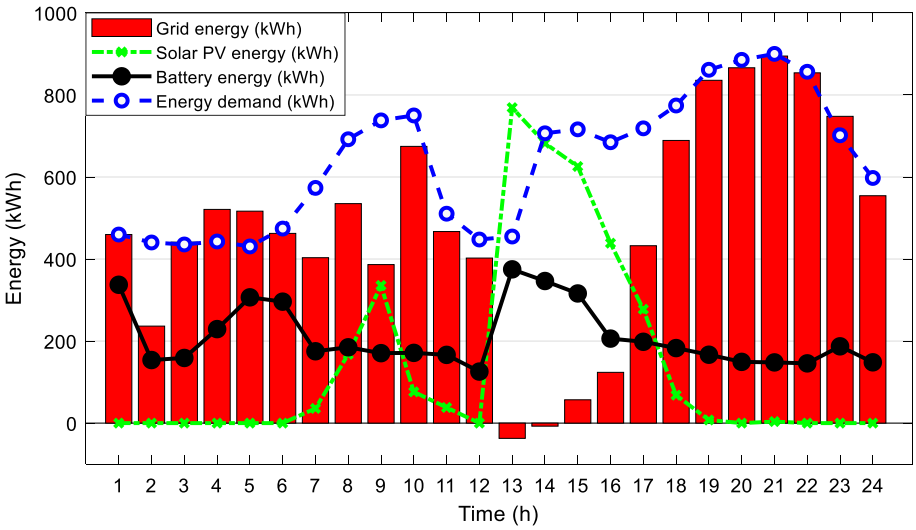

Fig. 18. FLB-PSO energy profile under fluctuating weather conditions.

the FLB-PSO algorithm to optimally operate loads on multiple energy sources, including solar PV and BESS, within a grid-connected framework. The proposed EMS addressed the limitations of independent heuristic optimization methods such as PSO in balancing exploration and exploitation in dynamic optimization problems. The solution demonstrated enhanced BESS utilization, improving overall system cost and efficiency. The three tested battery operational modes revealed that the algorithm effectively balanced grid power purchases and battery degradation costs. Mode 1, with 80 % battery SoC utilization capacity, incurs high grid cost and battery degradation. Mode 2, with 30 % battery SoC utilization capacity, incurs the highest grid and low battery degradation costs. The optimal Pareto was achieved with 50 % battery SoC utilization capacity, having the lowest grid utilization with moderately low battery degradation, resulting in the lowest daily operational cost.

Under dynamic tariff conditions, the FLB-PSO algorithm optimized battery charging during peak renewable generation periods, leading to significant cost savings and better operational efficiency for a long battery lifespan. The proposed algorithm also demonstrated superior performance in managing the hybrid EMS resources under fixed and dynamic grid tariffs, achieving quicker convergence and lower daily operational costs than conventional PSO. Overall, the FLB-PSO algorithm resulted in cost savings comparable to other advanced techniques, and the implementation was simpler and less computationally demanding compared to hybrid adaptive methods that rely on two iterative methods and machine learning. The algorithm proved highly effective, adaptive to process changes, and robust, achieving approximately 9–11 % savings in daily energy costs while ensuring optimal battery management and minimizing operational expenses. This was evident when tested under fluctuating weather conditions. Furthermore, this study underscores the potential significance of the proposed method as a strategic tool for microgrid operators, facilitating more intelligent decision-making in managing energy resources efficiently in sustainable power systems. Future research will investigate the algorithm's performance on new energy sources and integrate machine learning techniques and real-time data analytics to enhance the EMS adaptability and performance under more varying environmental conditions and load demands.

CRediT authorship contribution statement

Oladimeji Ibrahim: Writing – original draft, Methodology, Formal analysis. **Mohd Junaidi Abdul Aziz:** Conceptualization. **Razman Ayop:** Supervision, Formal analysis. **Ahmed Tijjani Dahiru:** Visualization, Validation. **Wen Yao Low:** Visualization. **Mohd Herwan Sulaiman:** Visualization. **Temitope Ibrahim Amosa:** Visualization, Validation.

Declaration of competing interest

The authors declare that they have no known competing financial interests or personal relationships that could have appeared to influence the work reported in this paper.

Data availability

Data will be made available on request.

Acknowledgment

The authors are thankful for the financial support through The Ministry of Higher Education under Universiti Teknologi Malaysia for the High-Tech Research Grant (F4) with vote number of Q. J130000.4623.00Q21 and Professional Development Research University Grant with vote number of Q.J130000.21A2.07E30.

References

[1] D. Gielen, F. Boshell, D. Saygin, M.D. Bazilian, N. Wagner, R. Gorini, The role of renewable energy in the global energy transformation, Energy Strategy Rev. 24 (2019) 38–50.
[2] IEA, Renewables 2023: Analysis and Forecast to 2028, 2023.
[3] Q. Hassan, S. Algburi, A.Z. Sameen, H.M. Salman, M. Jaszczur, A review of hybrid renewable energy systems: solar and wind-powered solutions: challenges, opportunities, and policy implications, Results in Engineering (2023) 101621.
[4] S.A. Qadir, H. Al-Motairi, F. Tahir, L. Al-Fagih, Incentives and strategies for financing the renewable energy transition: a review, Energy Rep. 7 (2021) 3590–3606.
[5] M. Khalid, Smart grids and renewable energy systems: perspectives and grid integration challenges, Energy Strategy Rev. 51 (2024) 101299.
[6] J. Liu, H. Wu, H. Huang, H. Yang, Renewable energy design and optimization for a net-zero energy building integrating electric vehicles and battery storage considering grid flexibility, Energy Convers. Manag. 298 (2023) 117768.
[7] H. Alghamdi, et al., A novel intelligent optimal control methodology for energy balancing of microgrids with renewable energy and storage batteries, J. Energy Storage 90 (2024) 111657.
[8] Y. Cui, Z. Geng, Q. Zhu, Y. Han, Multi-objective optimization methods and application in energy saving, Energy 125 (2017) 681–704.
[9] P. Mishra, G. Singh, Energy management systems in sustainable smart cities based on the internet of energy: a technical review, Energies 16 (19) (2023) 6903.
[10] A. Akter, et al., A review on microgrid optimization with meta-heuristic techniques: scopes, trends and recommendation, Energy Strategy Rev. 51 (2024) 101298.
[11] B. Jyoti Saharia, H. Brahma, N. Sarmah, A review of algorithms for control and optimization for energy management of hybrid renewable energy systems, J. Renew. Sustain. Energy 10 (5) (2018).

[12] X. Sun, H. He, L. Ma, Harmony search meta-heuristic algorithm based on the optimal sizing of wind-battery hybrid micro-grid power system with different battery technologies, J. Energy Storage 75 (2024) 109582.
[13] Y. Xu, et al., Optimization based on tabu search algorithm for optimal sizing of hybrid PV/energy storage system: effects of tabu search parameters, Sustain. Energy Technol. Assessments 53 (2022) 102662.
[14] M.G. Abdolrasol, R. Mohamed, M.A. Hannan, A.Q. Al-Shetwi, M. Mansor, F. Blaabjerg, Artificial neural network based particle swarm optimization for microgrid optimal energy scheduling, IEEE Trans. Power Electron. 36 (11) (2021) 12151–12157.
[15] C. Roy, D.K. Das, A hybrid genetic algorithm (GA)–particle swarm optimization (PSO) algorithm for demand side management in smart grid considering wind power for cost optimization, Sādhanā 46 (2) (2021) 101.
[16] Y. Duan, N. Chen, L. Chang, Y. Ni, S.S. Kumar, P. Zhang, CAPSO: chaos adaptive particle swarm optimization algorithm, IEEE Access 10 (2022) 29393–29405.
[17] G.S. Thirunavukkarasu, M. Seyedmahmoudian, E. Jamei, B. Horan, S. Mekhilef, A. Stojcevski, Role of optimization techniques in microgrid energy management systems—a review, Energy Strategy Rev. 43 (2022) 100899.
[18] S. Ruder, An Overview of Gradient Descent Optimization Algorithms, 2016 arXiv preprint arXiv:1609.04747.
[19] M.S. Daoud, M. Shehab, H.M. Al-Mimi, L. Abualigah, R.A. Zitar, M.K.Y. Shambour, Gradient-based optimizer (GBO): a review, theory, variants, and applications, Arch. Comput. Methods Eng. 30 (4) (2023) 2431–2449.
[20] H. Mataifa, S. Krishnamurthy, C. Kriger, Volt/var optimization: a survey of classical and heuristic optimization methods, IEEE Access 10 (2022) 13379–13399.
[21] S. Jamal, J. Pasupuleti, J. Ekanayake, A rule-based energy management system for hybrid renewable energy sources with battery bank optimized by genetic algorithm optimization, Sci. Rep. 14 (1) (2024) 4865.
[22] M. Restrepo, C.A. Cañizares, J.W. Simpson-Porco, P. Su, J. Taruc, Optimization-and rule-based energy management systems at the canadian renewable energy laboratory microgrid facility, Appl. Energy 290 (2021) 116760.
[23] H. Abdelhadi, A.M. Mahmoud, E.M.M. Saied, M.A.E. Mohamed, Innovative hierarchical control of multiple microgrids: cheetah meets PSO, Energy Rep. 11 (2024) 4967–4981.
[24] P. Barman, et al., Renewable energy integration with electric vehicle technology: a review of the existing smart charging approaches, Renew. Sustain. Energy Rev. 183 (2023) 113518.
[25] O. Ibrahim, et al., Development of fuzzy logic-based demand-side energy management system for hybrid energy sources, Energy Convers. Manag. X 18 (2023) 100354.
[26] V.V. Babu, J.P. Roselyn, P. Sundaravadivel, Multi-objective genetic algorithm based energy management system considering optimal utilization of grid and degradation of battery storage in microgrid, Energy Rep. 9 (2023) 5992–6005.
[27] M.A.E. Mohamed, A.M. Mahmoud, E.M.M. Saied, H.A. Hadi, Hybrid cheetah particle swarm optimization based optimal hierarchical control of multiple microgrids, Sci. Rep. 14 (1) (2024) 9313.
[28] M. Akorede, O. Ibrahim, S. Amuda, A. Otuoze, B. Olufeagba, Current status and outlook of renewable energy development in Nigeria, Nigerian Journal of Technology 36 (1) (2017) 196–212.
[29] PVGIS. "Photovoltaic Geographical Information System." European Commission (accessed.
[30] K. Ajao, R. Ambali, M. Mahmoud, Determination of the optimal tilt angle for solar photovoltaic panel in Ilorin, Nigeria, Journal of Engineering Science and Technology Review 6 (1) (2013) 87–90.
[31] K.S. El-Bidairi, H.D. Nguyen, S. Jayasinghe, T.S. Mahmoud, I. Penesis, A hybrid energy management and battery size optimization for standalone microgrids: a case study for Flinders Island, Australia, Energy Convers. Manag. 175 (2018) 192–212.
[32] T. Katrašnik, I. Mele, K. Zelič, Multi-scale modelling of Lithium-ion batteries: from transport phenomena to the outbreak of thermal runaway, Energy Convers. Manag. 236 (2021) 114036.
[33] J. Schmalstieg, S. Käbitz, M. Ecker, D.U. Sauer, A holistic aging model for Li (NiMnCo) O2 based 18650 lithium-ion batteries, J. Power Sources 257 (2014) 325–334.
[34] R. Peng, et al., Thermal runaway modeling of lithium-ion batteries at different scales: recent advances and perspectives, Energy Storage Mater. (2024) 103417.
[35] J.M. Mendel, Type-1 fuzzy sets and fuzzy logic, in: Explainable Uncertain Rule-Based Fuzzy Systems, Springer, 2024, pp. 17–73.
[36] W. a. A. K. Cole. Cost Projections for Utility-Scale Battery Storage: 2023 Update. Golden, CO: National Renewable Energy Laboratory. NREL/TP-6A40-85332 https://www.nrel.gov/docs/fy23osti/85332.pdf.
[37] M.M. Kamal, I. Ashraf, Evaluation of a hybrid power system based on renewable and energy storage for reliable rural electrification, Renewable Energy Focus 45 (2023) 179–191.
[38] İ. ÇetınbaŞ, B. Tamyürek, M. Demırtaş, The hybrid harris hawks optimizer-arithmetic optimization algorithm: a new hybrid algorithm for sizing optimization and design of microgrids, IEEE Access 10 (2022) 19254–19283.
[39] K. Zhao, K. He, Z. Liang, M. Mai, Global optimization-based energy management strategy for series–parallel hybrid electric vehicles using multi-objective optimization algorithm, Automotive Innovation 6 (3) (2023) 492–507.